

Modeling The Effects of Leakage Inductance On Flyback Converters (Part 3): The Small-Signal Model

by Christophe Basso, ON Semiconductor, Toulouse, France

In the final part of this article series, we will study the small-signal response of the CCM flyback converter operated in voltage mode as influenced by the leakage inductance. From the updated large-signal model introduced in part 2, we will progress step-by-step through successively-simplified small-signal schematics with the goal of establishing the simplest linear version. From this final circuit, we will extract a control-to-output transfer function that shows how the leakage inductance affects the quality factor of the transfer function denominator.

From Large To Small Signal

When you derive the transfer function of a complicated circuit, your aim is to reduce complexity so that analysis is performed on the simplest schematic. However, as you progress through the circuit reduction—by factoring terms, simplifying expressions, neglecting variables and so on—you must test your new circuit and compare its response to that of the original circuit, the one at the beginning of the exercise. Any deviation between the original response and what your next simplified version delivers indicates that you made a mistake or the assumption you made is overly simplistic: Discard the circuit and go back one step to rework it.

By following these steps, you progress slowly but surely as you immediately detect and correct mistakes. Experience teaches that nothing is more frustrating than identifying an error at the very end when you realize something was wrong in one of the intermediate steps!

The first thing we can do is replace the large-signal PWM switch model with its small-signal version, which was introduced in part 2. Then, we can run an ac simulation and verify that operating points and responses are identical. The non-linear (i.e. large-signal) model is shown in Fig. 1 while the small-signal version appears in Fig. 2.

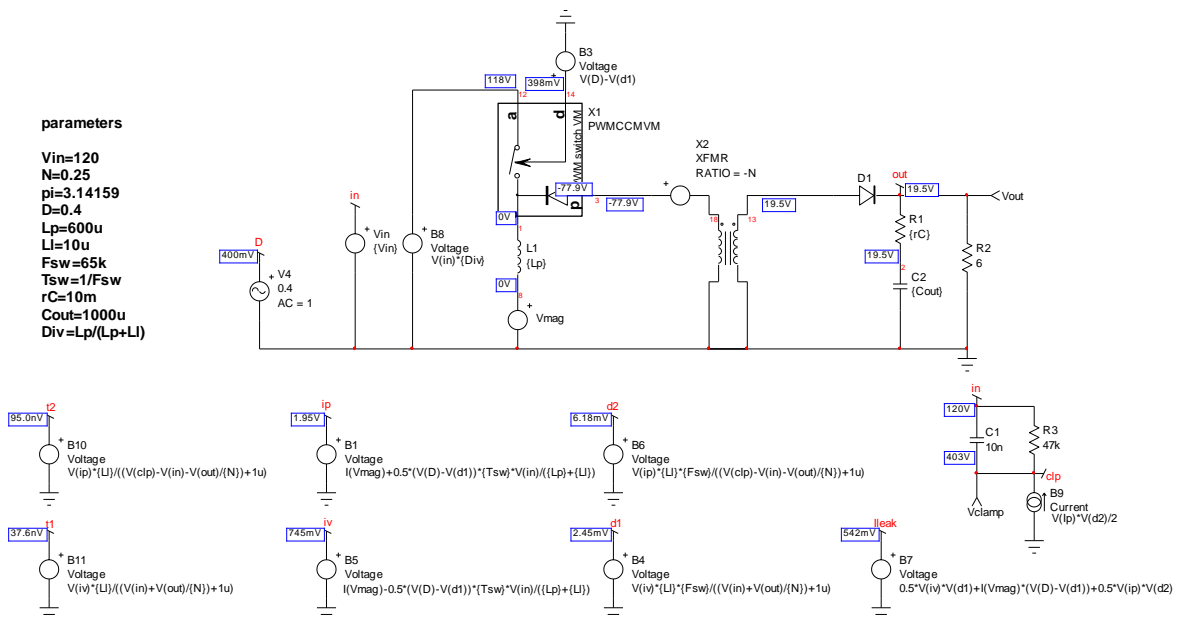


Fig. 1. This open-loop large-signal schematic is our starting circuit for analysis and its dynamic response will serve as a reference in the following steps.

The duty ratio has been split into two sources, one for the static duty ratio and a second for the ac modulation; the \hat{d} in the small-signal equations. Bias points are identical to those of Fig. 1, meaning that this first step is correct, dc-wise. Let's check how the frequency responses of these two circuits compare. We have gathered Bode plots in Fig. 3: magnitude and phase curves superimpose, validating our first step.

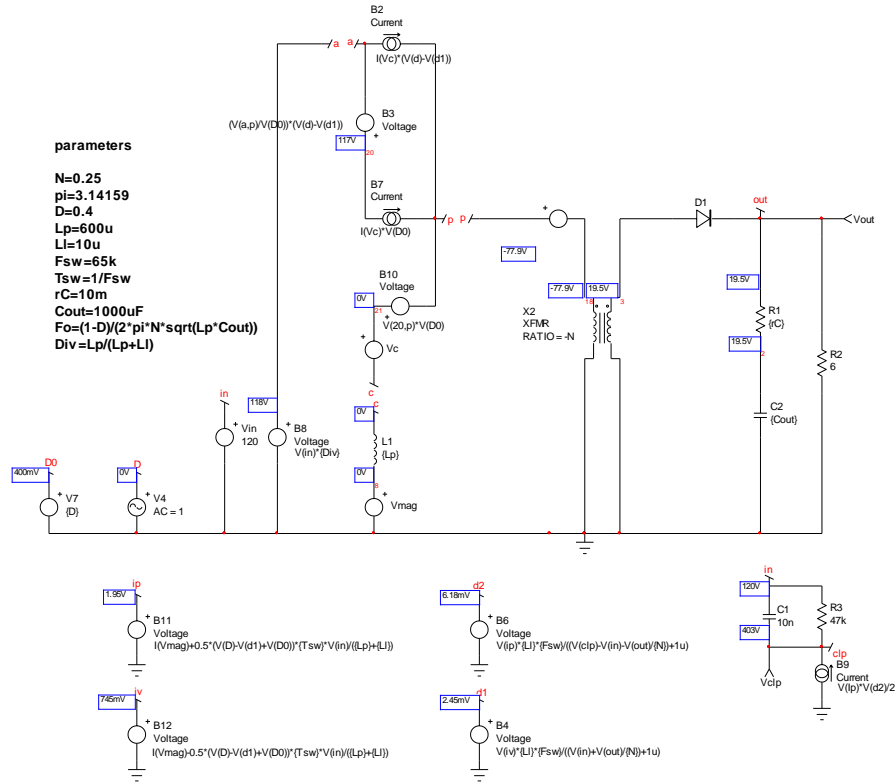


Fig. 2. The PWM switch is replaced by its small-signal version and the circuit dynamic response is checked against the reference frequency response.

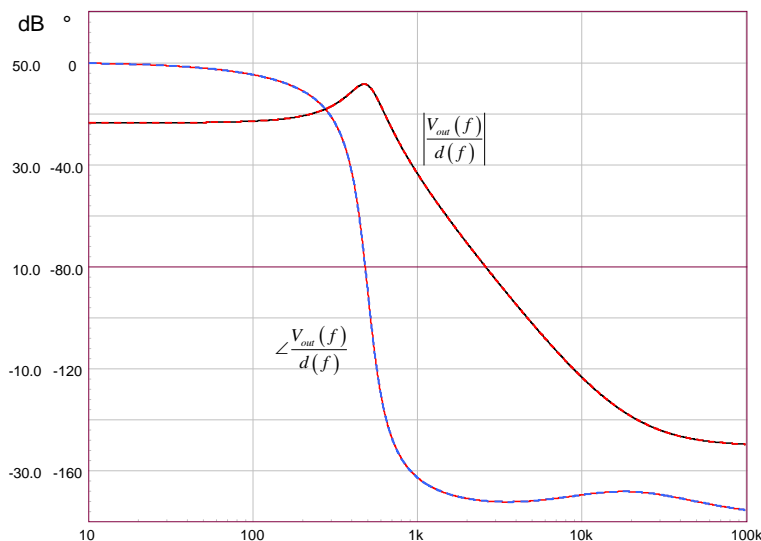


Fig. 3. Bode plots of both circuits perfectly superimpose, validating this first step.

The circuit in Fig. 2 is correct but quite complicated. As stated, small-signal analysis implies simplifying the circuit as much as you can and rearranging the various components into a more meaningful architecture. Please note that V_c and V_{mag} are dummy 0-V sources and probe the current leaving terminal "c".

The PWM switch model we plugged in is indeed a linearized version and we do not need to work on it. However, all the sources computing the peak and valley currents, the clamp voltage and so on are still large-signal expressions that we need to linearize. Fortunately, some of these sources are not needed in our ac analysis such as I_p and d_2 for instance.

Linearization Of Sources

You have two options if you want to linearize these sources. You can perturb each variable with a small excitation—the little hat $\hat{}$ you see on certain variables—and sort out ac and dc terms to form two separate equations: a static and a dynamic expression. The static expression describes the operating point while the dynamic expression is the one we want.

The problem with this technique is the number of terms and cross products you obtain, especially with more than two variables. Sorting these terms for forming ac and dc equations can sometimes be tedious and lead to mistakes. To illustrate, let's try with the valley current definition:

$$I_v = I_c - \frac{(d - d_1)V_{in}T_{sw}}{2(l_{leak} + L_p)} \quad (1)$$

There are three variables here, I_c , d and d_1 . If we perturb each variable with a small quantity, we have

$$I_v + \hat{i}_v = I_c + \hat{i}_c - \frac{(d + \hat{d} - d_1 - \hat{d}_1)V_{in}T_{sw}}{2(l_{leak} + L_p)} \quad (2)$$

Expanding leads to

$$I_v + \hat{i}_v = I_c + \hat{i}_c + d_1 \frac{T_{sw}V_{in}}{2(L_p + l_{leak})} - d \frac{T_{sw}V_{in}}{2(L_p + l_{leak})} + \hat{d}_1 \frac{T_{sw}V_{in}}{2(L_p + l_{leak})} - \hat{d} \frac{T_{sw}V_{in}}{2(L_p + l_{leak})} \quad (3)$$

Now collecting ac and dc terms, we have two definitions:

$$I_v = I_c + d_1 \frac{T_{sw}V_{in}}{2(L_p + l_{leak})} - d \frac{T_{sw}V_{in}}{2(L_p + l_{leak})} \quad (4)$$

$$\hat{i}_v = \hat{i}_c + \hat{d}_1 \frac{T_{sw}V_{in}}{2(L_p + l_{leak})} - \hat{d} \frac{T_{sw}V_{in}}{2(L_p + l_{leak})}$$

If we define two coefficients k_{ivd} and k_{ivd1} as

$$k_{ivd} = - \frac{T_{sw}V_{in}}{2(L_p + l_{leak})} \quad (5)$$

$$k_{ivd1} = \frac{T_{sw} V_{in}}{2(L_p + I_{leak})} \quad (6)$$

then the dynamic equation in (4) can be rearranged in a simpler format

$$\hat{i}_v = \hat{i}_c + \hat{d}_1 k_{ivd1} + \hat{d} k_{ivd} \quad (7)$$

Static coefficients k_{ivd} and k_{ivd1} will be passed as parameters in the schematic capture and evaluated before simulation begins.

The triage operation was simple here but with complex expressions and multiple variables, it quickly becomes a difficult exercise that you cannot automate under a solver like Mathcad. A faster way consists of using partial differentiations given a set of uncorrelated (independent) variables as shown below:

$$di_v = \frac{\partial I_v(I_c, d, d_1)}{\partial I_c} di_c + \frac{\partial I_v(I_c, d, d_1)}{\partial d_1} dd_1 + \frac{\partial I_v(I_c, d, d_1)}{\partial d} dd \quad (8)$$

or using small-signal notation

$$\hat{i}_v = \frac{\partial I_v(I_c, d, d_1)}{\partial I_c} \hat{i}_c + \frac{\partial I_v(I_c, d, d_1)}{\partial d_1} \hat{d}_1 + \frac{\partial I_v(I_c, d, d_1)}{\partial d} \hat{d} \quad (9)$$

Here, coefficients for ac terms only are obtained from these partial differentiations. Applying this method to the d_1 generator in Fig. 2 gives

$$\hat{d}_1 = \frac{\partial d_1(I_v, V_{out})}{\partial I_v} \hat{i}_v + \frac{\partial d_1(I_v, V_{out})}{\partial V_{out}} \hat{v}_{out} \quad (10)$$

which leads to evaluating

$$\hat{d}_1 = \frac{\partial}{\partial V_{out}} \frac{I_v I_{leak} F_{sw}}{V_{in} + \frac{V_{out}}{N}} \hat{v}_{out} + \frac{\partial}{\partial I_v} \frac{I_v I_{leak} F_{sw}}{V_{in} + \frac{V_{out}}{N}} \hat{i}_v \quad (11)$$

Considering k_{d1vo} and k_{d1iv} coefficients, we can rewrite equation 11 as

$$\hat{d}_1 = k_{d1vo} \hat{v}_{out} + k_{d1iv} \hat{i}_v \quad (12)$$

in which

$$k_{d1vo} = - \frac{F_{sw} I_v I_{leak}}{N \left(V_{in} + \frac{V_{out}}{N} \right)^2} \quad (13)$$

$$k_{d1iv} = \frac{F_{sw} I_{leak}}{V_{in} + \frac{V_{out}}{N}} \quad (14)$$

Now that we have linearized d_1 and I_V sources, we can update and simplify the Fig. 2 circuit. The result appears in Fig. 4: the parameters defined in equations 5 and 6 and in 13 and 14 are calculated in the parameters text window. All sources in this diagram are now small-signal types. A quick ac analysis shows that the frequency response in magnitude and phase exactly matches that of Fig. 3.

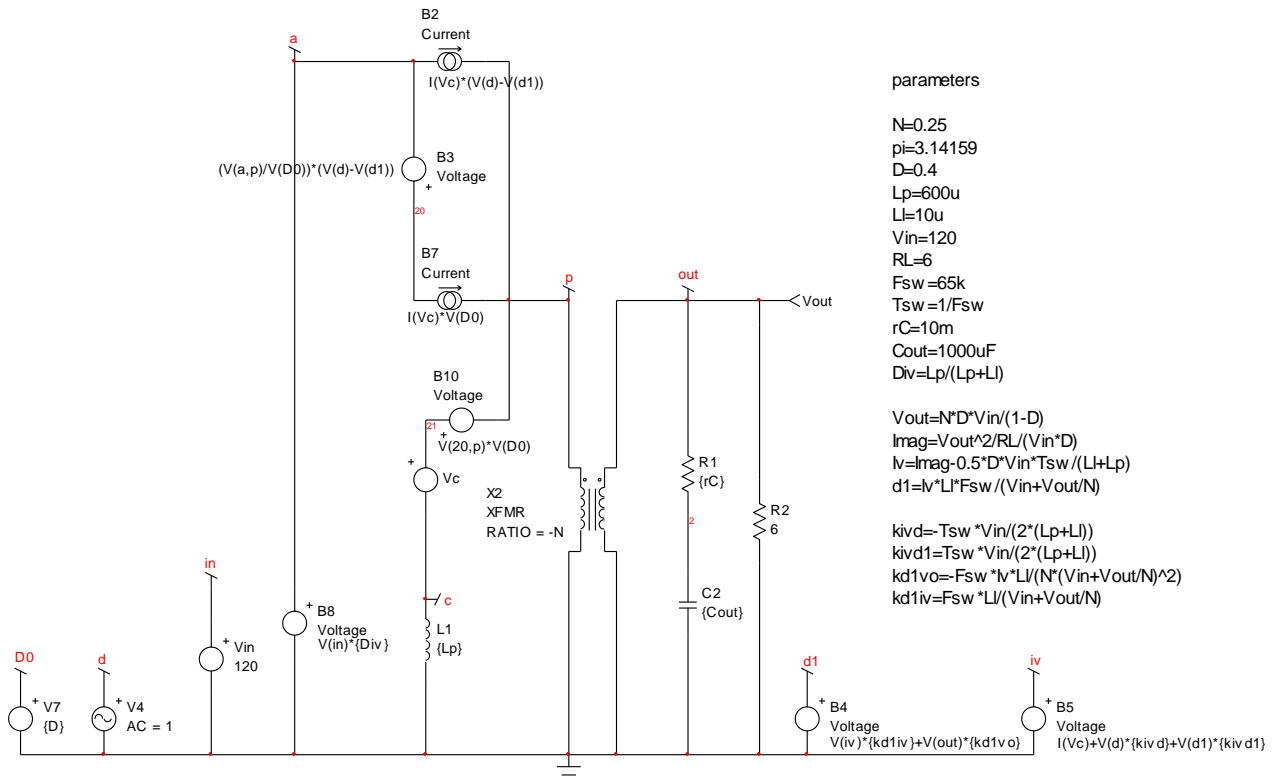


Fig. 4. The updated circuit now includes linearized sources only.

Simplifying The Schematic

We could start analyzing the linearized converter from the schematic in Fig. 4. However, further simplifications and rearrangements are possible. For instance, in the control-to-output transfer function, the input voltage V_{in} is constant, meaning that \hat{v}_{in} or $V_{in}(s)$ are equal to 0. As such, node "a" which is connected to the input voltage can be advantageously grounded. By grounding node "a", you can redraw the circuit and reveal a simpler version as shown in Fig. 5. The frequency response of this circuit is tested against that of Fig. 3 to detect any errors in the newly-arranged model.

Further observation shows that current source B_7 is in series with voltage source B_1 . For the sake of simplifying further, B_7 negative terminal can be ground-referenced while B_1 is transformed into a separate source with its output connected to node 20. The new circuit is given in Fig. 6.

Next, we observe that node 20 is used in the B_{10} source (which is updated with its definition) and both current sources B_7/B_2 can be paralleled to form a single source. This is what is shown in Fig. 7 as a final circuit for the analysis.

Please note that the expression for source I_V has been included in the d_1 source. The frequency response of this circuit is plotted versus that of the large-signal reference model in Fig. 8. As phase and magnitude responses are identical, we can now work on this final representation.

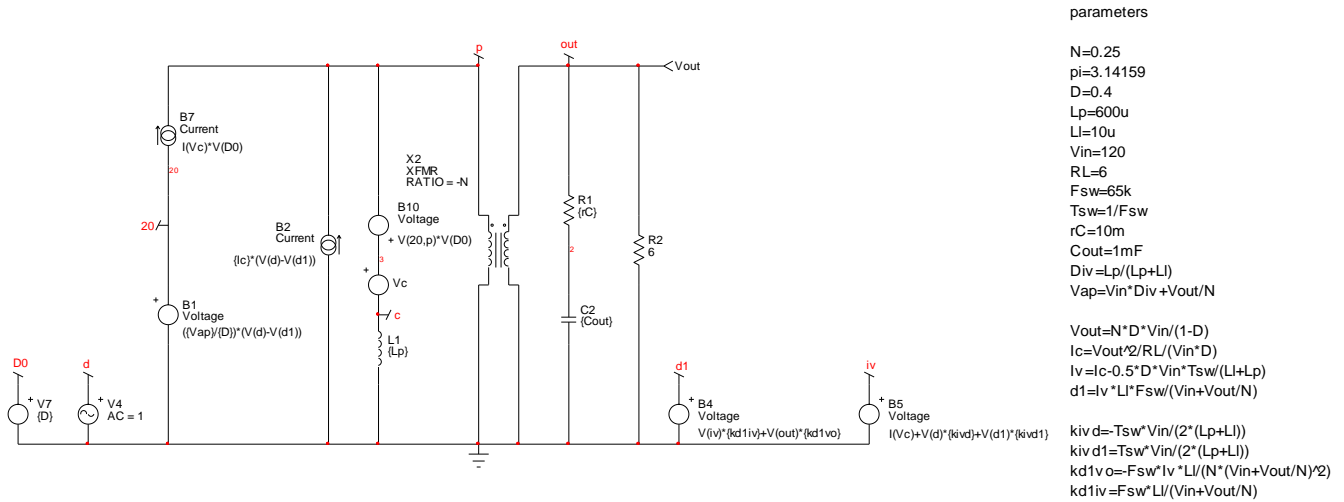


Fig. 5. Considering a constant input voltage, node "a" in Fig. 4 can be grounded and further simplification brought to the small-signal circuit.

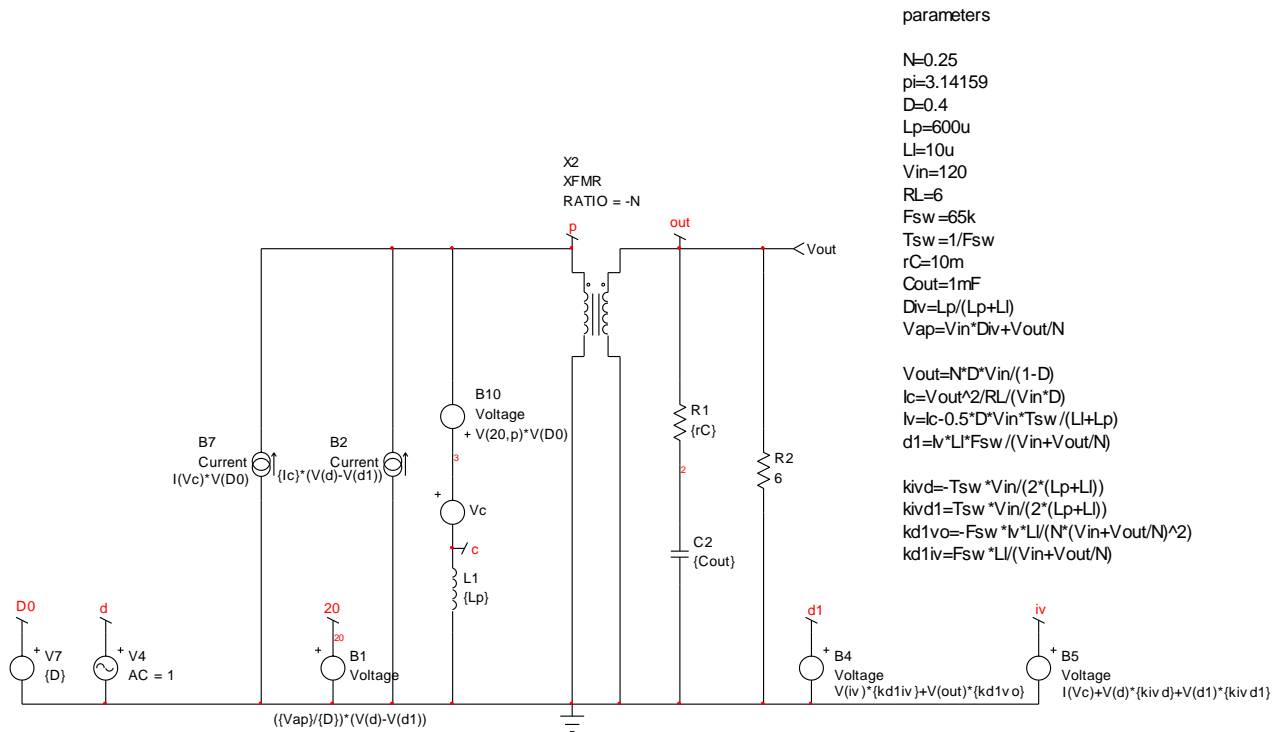


Fig. 6. Current source B_7 is now grounded while B_1 delivers its voltage at node 20. V_c is a 0-V dummy source probing the current in the primary inductance.

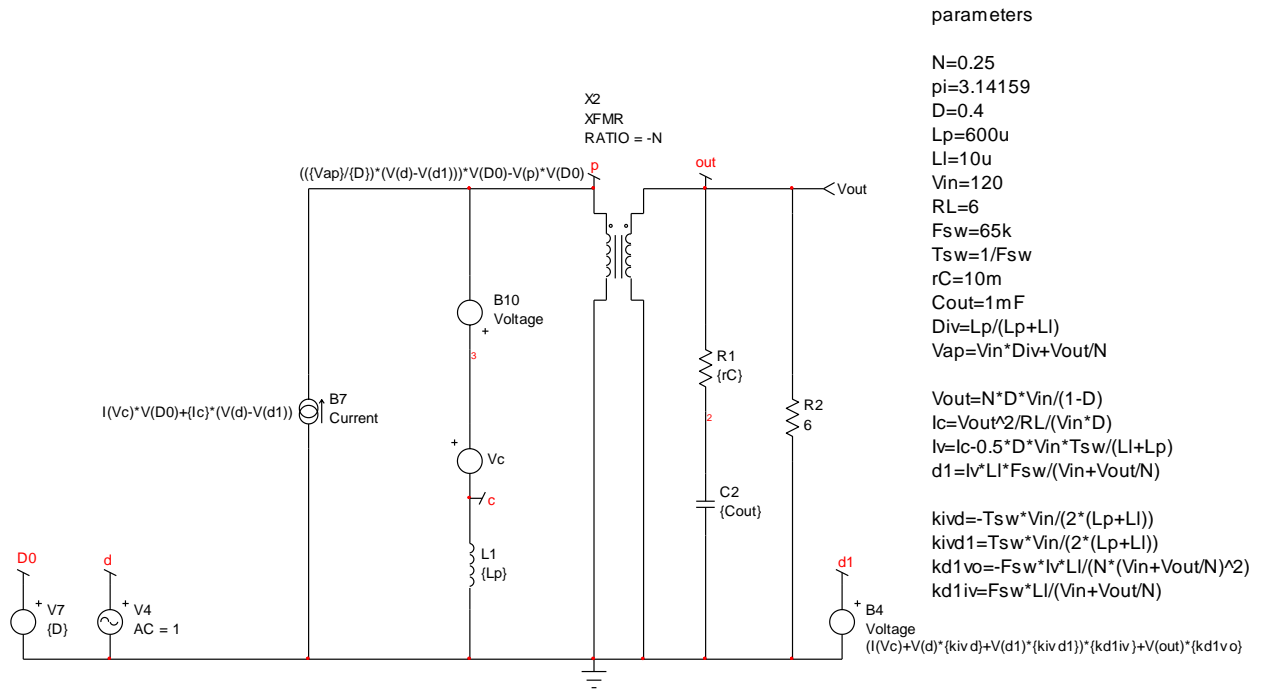


Fig. 7. Once current source B_2 in Fig. 6 has been incorporated into B_7 and node 20 has been integrated into B_{10} , we have our final small-signal schematic. I_v has been incorporated into d_1 .

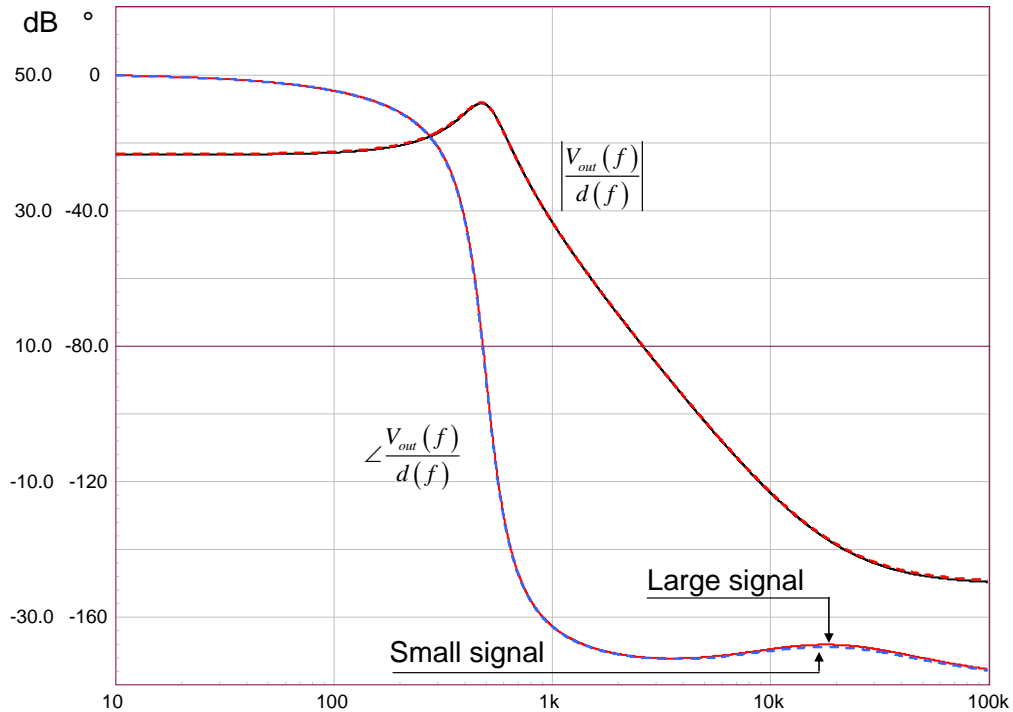


Fig. 8. The frequency response of the large-signal model (solid lines) and that of our simplified circuit from Fig. 7 (dotted lines) are identical.

Generating The Equations

We start by observing that the inductor current is equal to the voltage at node "c" divided by the inductor impedance. The voltage at node "c" is defined by the voltage at node "p" in series with voltage source B₁₀. The voltage at node "p" is simply minus the output voltage reflected to the primary side via the transformer turns ratio N (neglecting the diode forward drop). So, we have

$$I_L(s) = \frac{V_{(c)}}{sL_p} = \frac{-\frac{V_{out}(s)}{N} + V_{ap} [d(s) - d_1(s)] D_0 + \frac{V_{out}(s)}{N} D_0}{sL_p} \quad (15)$$

Source d_1 can be rewritten since the current in L_p is now defined (it is $I(V_c)$ in the d_1 source from Fig. 7)

$$d_1(s) = \left[\frac{-\frac{V_{out}(s)}{N} + V_{ap} [d(s) - d_1(s)] D_0 + \frac{V_{out}(s)}{N} D_0}{sL_p} + d(s) \cdot k_{ivd} + d_1(s) \cdot k_{ivd1} \right] k_{d1iv} + V_{out}(s) k_{d1vo} \quad (16)$$

Solving for $d_1(s)$ leads to

$$d_1(s) = \frac{D_0 V_{out}(s) k_{d1iv} - V_{out}(s) k_{d1iv} + D_0 N V_{ap} d(s) k_{d1iv} + s N L_p (V_{out}(s) k_{d1vo} + d(s) k_{ivd} k_{d1iv})}{s N L_p (1 - k_{d1iv} k_{ivd1}) + D_0 N V_{ap} k_{d1iv}} \quad (17)$$

The output current is the primary current scaled by the transformer turns ratio N . It is the current defined by source B₇ minus the current flowing in the inductor, which is defined by equation 15:

$$I_{out}(s) = \frac{\left[\frac{-\frac{V_{out}(s)}{N} + V_{ap} [d(s) - d_1(s)] D_0 + \frac{V_{out}(s)}{N} D_0}{sL_p} \right] (D_0 - 1) + I_c [d(s) - d_1(s)]}{N} \quad (18)$$

In this expression, I_c is a dc value already determined in part 2 of this article series

$$I_c = \frac{V_{out}^2}{R_L \cdot d \cdot V_{in}} \quad (19)$$

The I_{out} current circulates in an impedance consisting of r_C , C_{out} and the load resistance R_L as shown in Fig. 9.

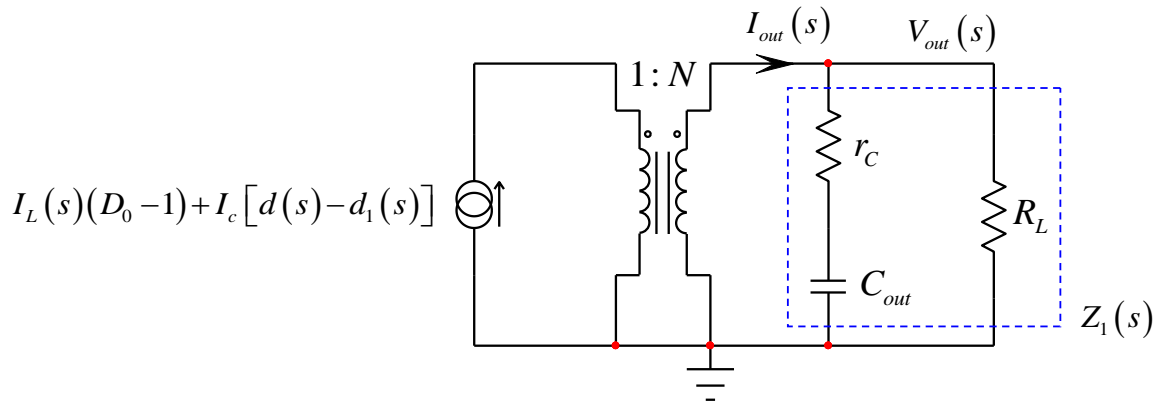


Fig. 9. A more compact representation of the small-signal model includes a transformer driving a complex impedance made of the output capacitor, its ESR and the load resistance R_L .

This output current can also be defined as

$$I_{out}(s) = \frac{V_{out}(s)}{Z_1(s)} \quad (20)$$

Impedance Z_1 can be derived quickly either by paralleling $r_C + C_{out}$ with R_L or applying Fast Analytical Circuits Techniques (FACTs). Using either approach, when the result is rearranged you should find

$$Z_1(s) = R_L \frac{1 + sr_C C_{out}}{1 + s(r_C + R_L)C_{out}} \quad (21)$$

Now combining equations 18, 20 and 21, we can write

$$\frac{\left[\frac{-\frac{V_{out}(s)}{N} + V_{ap}[d(s) - d_1(s)]D_0 + \frac{V_{out}(s)}{N}D_0}{sL_p} \right] (D_0 - 1) + I_c[d(s) - d_1(s)]}{N} = \frac{V_{out}(s)}{R_L \frac{1 + sr_C C_{out}}{1 + s(r_C + R_L)C_{out}}} \quad (22)$$

The fun now lies in solving for V_{out} and rearranging the transfer function in a second-order polynomial form. With the help of Mathcad, we obtain:

$$\frac{V_{out}(s)}{d(s)} = H_0 \frac{\left(1 + \frac{s}{\omega_{z_1}}\right) \left(1 - \frac{s}{\omega_{z_2}}\right)}{1 + b_1 s + b_2 s^2} = H_0 \frac{\left(1 + \frac{s}{\omega_{z_1}}\right) \left(1 - \frac{s}{\omega_{z_2}}\right)}{1 + \frac{s}{\omega_0 Q} + \left(\frac{s}{\omega_0}\right)^2} \quad (23)$$

in which we have determined the following raw coefficients.

$$H_0 := \frac{[N_1(k_{ivd}k_{diiv} + k_{diiv}k_{ivd} - 1)][V_{ap}(1 - D_0)]}{\left[(2D_0 - D_0^2 - I_c k_{diiv} + k_{diiv}k_{ivd} - 2D_0 k_{diiv}k_{ivd} + D_0^2 k_{diiv}k_{ivd} + D_0 I_c k_{diiv} - N_1 V_{ap} k_{diiv} + D_0 N_1 V_{ap} k_{diiv} - 1) - \frac{N_1^2 V_{ap} k_{diiv}}{R_L} \right]}$$

$$b_1 := \frac{V_{ap} [N_1^2 [L_p - L_p k_{diiv}k_{ivd} + V_{ap} k_{diiv} (C_{out} R_L + C_{out} r_C)] - R_L [C_{out} r_C (2D_0 - D_0^2 - I_c k_{diiv} + k_{diiv}k_{ivd} - 2D_0 k_{diiv}k_{ivd} + D_0^2 k_{diiv}k_{ivd} + D_0 I_c k_{diiv} - N_1 V_{ap} k_{diiv} + D_0 N_1 V_{ap} k_{diiv} - 1) + I_c L_p N_1 k_{diiv}]] (D_0 - 1)}{V_{ap} (1 - D_0) [R_L (2D_0 - D_0^2 - I_c k_{diiv} + k_{diiv}k_{ivd} - 2D_0 k_{diiv}k_{ivd} + D_0^2 k_{diiv}k_{ivd} + D_0 I_c k_{diiv} - N_1 V_{ap} k_{diiv} + D_0 N_1 V_{ap} k_{diiv} - 1) - N_1^2 V_{ap} k_{diiv}]}$$

$$b_2 := \frac{[D_0 V_{ap} (D_0 - 1) [N_1^2 (C_{out} R_L + C_{out} r_C) (L_p - L_p k_{diiv}k_{ivd}) - C_{out} I_c L_p N_1 R_L k_{diiv} r_C]]}{[D_0 V_{ap} (1 - D_0) [R_L (2D_0 - D_0^2 - I_c k_{diiv} + k_{diiv}k_{ivd} - 2D_0 k_{diiv}k_{ivd} + D_0^2 k_{diiv}k_{ivd} + D_0 I_c k_{diiv} - D_0 N_1 V_{ap} k_{diiv} + D_0^2 N_1 V_{ap} k_{diiv} - 1) - D_0 N_1^2 V_{ap} k_{diiv}]}$$

$$\omega_{z1} := \frac{1}{r_C C_{out}} \quad \omega_{z2} := \frac{V_{ap}(1 - D_0)}{(L_c L_p)} \quad Q := \frac{\sqrt{b_2}}{b_1} \quad \omega_0 := \frac{1}{\sqrt{b_2}}$$

The transfer function (without leakage inductance) given in the literature for the classical CCM-operated voltage-mode flyback converter follows the form of equation 23 and uses the definitions below:

$$H_0 = \frac{NV_{in}}{(1 - D)^2} \quad \omega_{z1} = \frac{1}{r_C C_{out}} \quad \omega_{z2} = \frac{(1 - D)^2 R_L}{DL_p N^2}$$

$$Q = \frac{1 - D}{N} R_L \sqrt{\frac{C_{out}}{L_p}} \quad \omega_0 = \frac{1 - D}{N \cdot \sqrt{L_p C_{out}}}$$

Testing Analytical Expressions

If we assume the operating values from Fig. 1 and plot the response given by equation 23 considering either the complicated coefficients with a zero I_{leak} ($r_C = 0 \Omega$) or the simplified flyback expression, both magnitude and phase response plots perfectly superimpose as represented in Fig. 10.

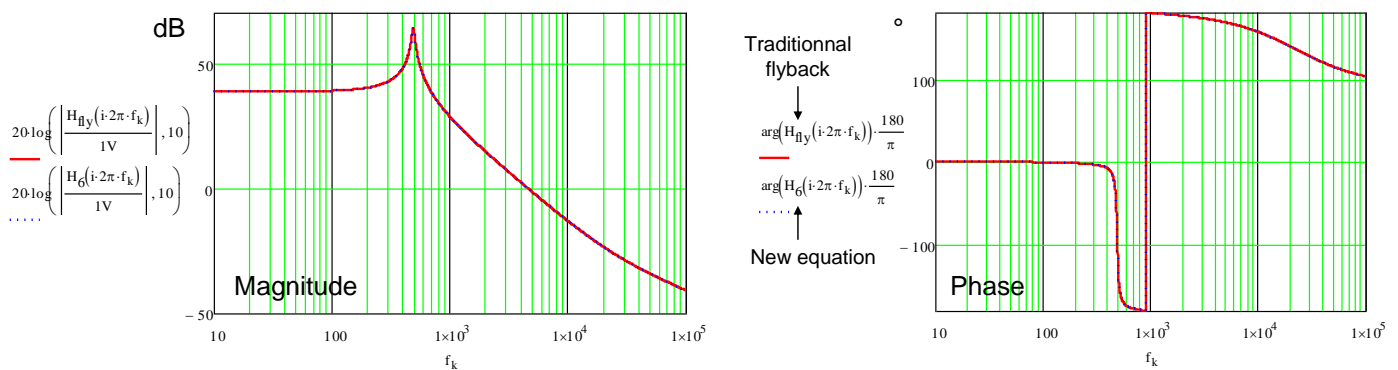


Fig. 10. When the leakage inductance is set to zero, the equation with complex coefficients and the traditional flyback expression return the same frequency response plots.

The next test consists of setting I_{leak} to 10 μ H and superimposing the plots obtained from Mathcad and the small-signal SPICE simulation. As shown by Fig. 11, the perfect superimposition of curves confirms our mathematical derivation of the transfer function considering the leakage inductance.

Finally, to compare our modeling approach with another simulation platform, my colleague Dr. Capilla captured the simplified cycle-by-cycle model introduced in part 1 in a Simplis template (Fig. 12) and ran several

configurations to extract the small-signal response. Results appear in Fig. 13 over which we have pasted the SPICE simulation results obtained with the small-signal model.

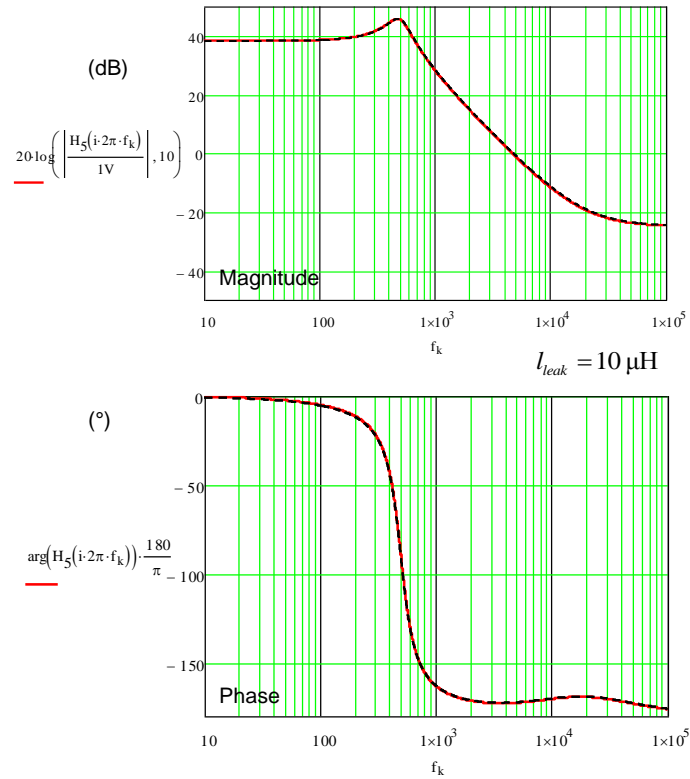


Fig. 11. SPICE and Mathcad plots superimpose perfectly, confirming our analytical derivation of the transfer function linking d to V_{out} in Fig. 4.

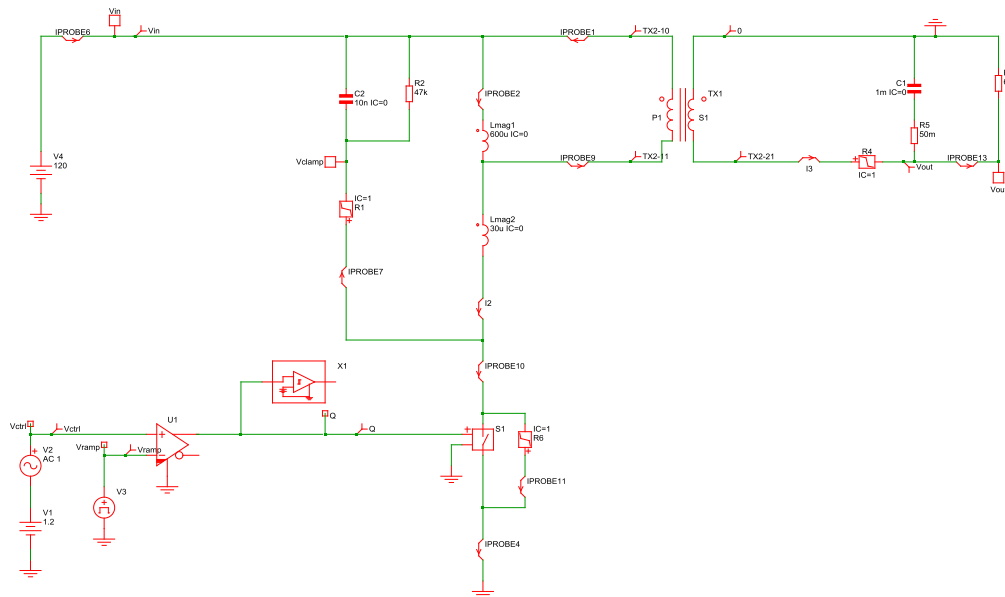


Fig. 12. Simplis can extract the small-signal response from a switching circuit.

© 2016 How2Power. All rights reserved.

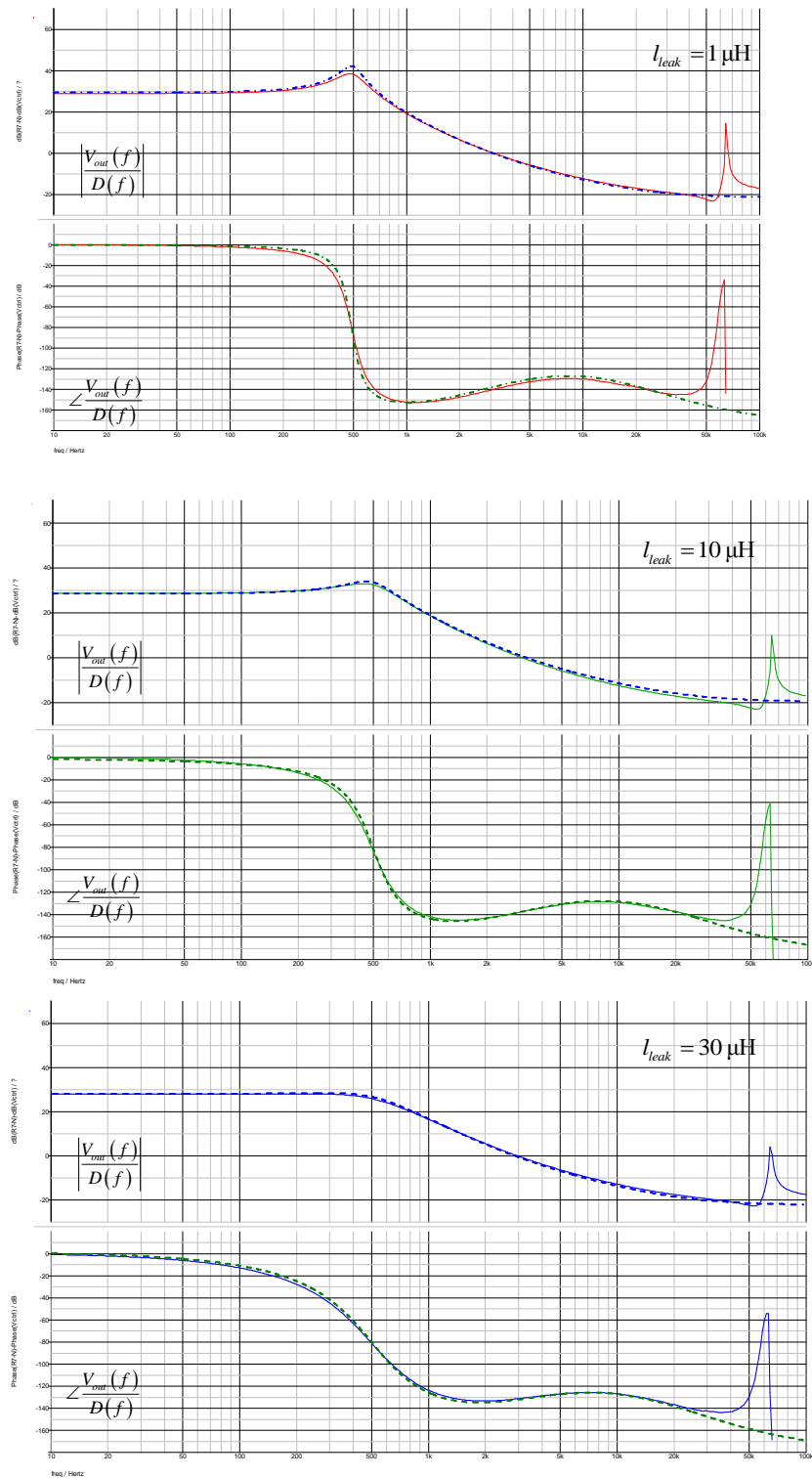


Fig. 13. Dynamic responses from Simplis (solid lines) show a slightly damped circuit compared to the SPICE averaged model (dotted lines). The high-frequency peaks are an artifact linked to the 65-kHz switching frequency.

For the 1- μH leakage inductance value, Simplis shows a slightly lower Q , probably due to losses inherent to some of the selected switching elements in the simulated circuit. For higher leakage inductance values (10 and 30 μH), the agreement is very good and curves almost superimpose.

Leakage Inductance And Quality Factor

Now that our model is correct, we can ac-sweep the Fig. 1 circuit and see how magnitude and phase curves are affected by the leakage inductance. With a low leakage inductance, the Q is significant and exceeds 10 dB. As the leakage inductance grows, more energy is lost per switching cycle and the quality factor weakens. For a large inductance value, 30 μH , the system becomes overdamped.

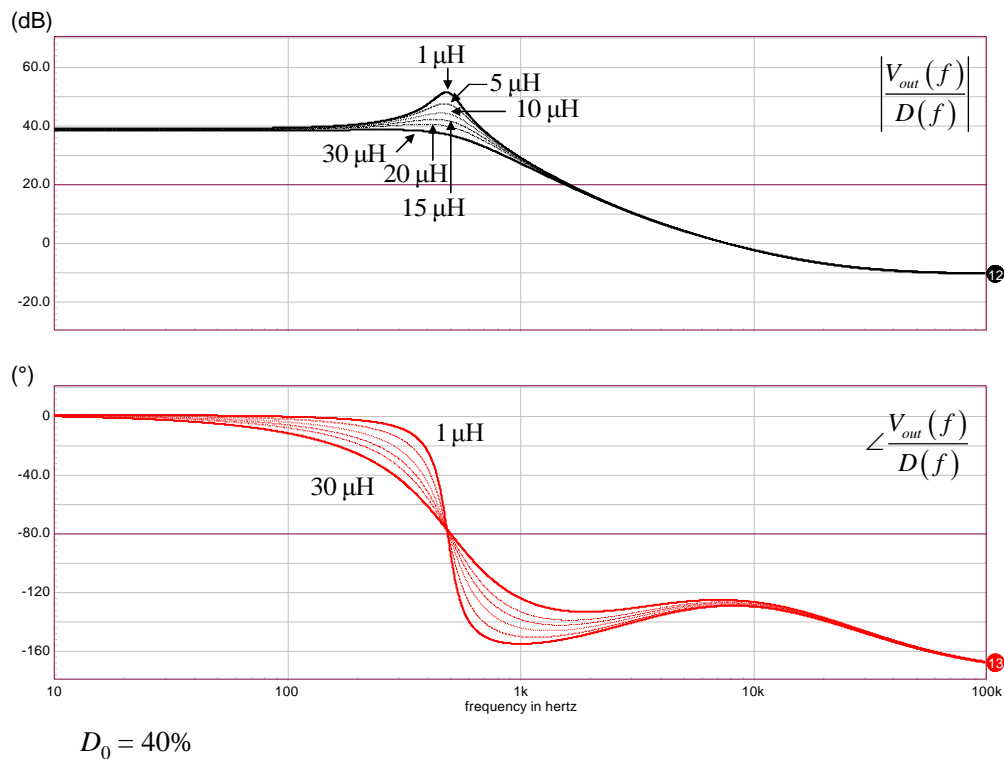


Fig. 14. Increasing the leakage inductance clearly damps the response of the CCM flyback converter operated in voltage mode.

In Fig. 15, we have plotted Q versus the leakage inductance value, confirming its damping effect on the flyback converter.

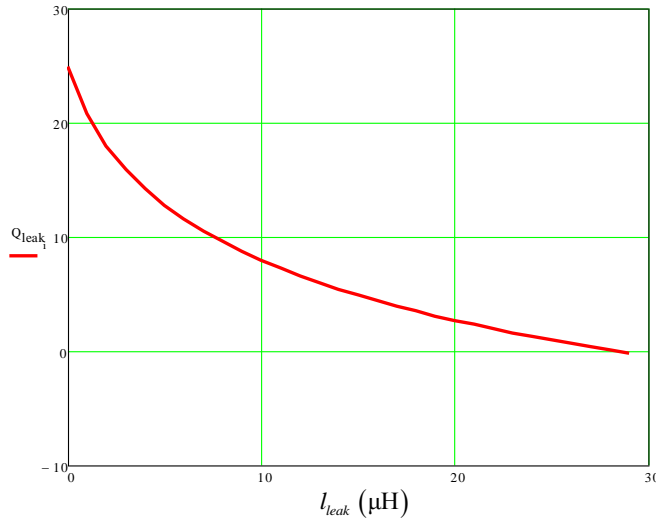


Fig. 15. The quality factor in dB reduces as the leakage inductance increases.

In current mode, the duty ratio truncation disappears because despite the inclusion of the leakage inductance, the peak current remains unaffected as t_{on} naturally expands to meet the peak setpoint. As derived in reference 1 (page 199), it is possible to show that the switch duty ratio in current mode control (CCM) is defined by

$$d = \frac{F_{sw} (V_c - R_i I_c)}{S_a + \frac{V_{ac} R_i}{2(L_p + l_{leak})}} \quad (24)$$

in which F_{sw} is the switching frequency, V_c is the control voltage, R_i the sense resistance, I_c the current in terminal "c" as defined by equation 19, S_a the external compensation ramp in V/s and V_{ac} the voltage between terminals "a" and "c". Despite the increase of the leakage inductance, the effective duty ratio (the switch duty ratio reduced by the leakage inductance magnetization time) remains fairly constant. As such, it is mostly the delay in the secondary current that affects the output voltage. However, the output voltage reduction in current-mode control is still lower than that of the voltage-mode converter (Fig. 16.)

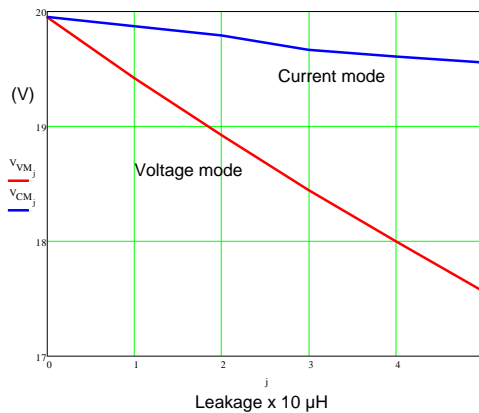


Fig. 16. In current mode, the peak current remains constant and the on-time naturally expands to compensate for the presence of leakage inductance. As a result, the output voltage is almost unaffected unlike in voltage-mode control.

Conclusion

In this final part, we have expressed the control-to-output transfer function of the CCM flyback converter operated in voltage mode. The leakage inductance increases the dissipation in the clamping source and provides damping of the frequency response: classical equations do not predict this behavior and a new model had to be derived.

Starting from a large-signal model, we have linearized the model in several steps to obtain a new small-signal model that includes the effects of leakage inductance. From this model, a new small-signal transfer function has been established, showing the leakage inductance effect on the quality factor. Current-mode control, however, is less affected by the leakage inductance. References 2 and 3 point to papers recognizing the influence of the leakage element without formalizing its effect in an updated transfer function expression.

The leakage inductance small-signal effects in a classical hard-switching converter are not of great importance. However, analyzing mechanisms at work paves the way for the study of a more-complex architecture, the active-clamp flyback converter. In this structure, the leakage inductance is purposely used to defeat switching losses inherent to the drain-source lumped capacitance. As we will see in an upcoming series of articles, duty ratio truncation increases as the leakage inductance current no longer starts from zero but from a negative value.

References

1. "Switch Mode Power Supplies: SPICE Simulations and Practical Designs," second edition by C. Basso, McGraw-Hill 2014, ISBN 978-0071823463.
2. "Analysis of Leakage Inductance Effect on Characteristics of Flyback Converter Without Right Half Plane Zero" by H. Terashi and T. Ninomiya, Power Electronics and Motion Control Conference, 2004 (IPEMC 2004), Vol. 3.
3. "Unified Flyback Switching-Cell Model Including the Leakage Inductance Effects for SPICE Simulation" by K. Rustom et al., Power Electronics Specialist Conference, 2003 (PESC '03).

About The Author



Christophe Basso is a technical fellow at ON Semiconductor in Toulouse, France. He has originated numerous integrated circuits among which the NCP120X series has set new standards for low standby power converters. SPICE simulation is also one of his favorite subjects and he has authored two books on the subject. Christophe's latest work is "Designing Control Loops for Linear and Switching Power Supplies: A Tutorial Guide."

Christophe received a BSEE-equivalent from the Montpellier University, France and an MSEE from the Institut National Polytechnique de Toulouse, France. He holds 18 patents on power conversion and often publishes papers in conferences and trade magazines.

For further reading on leakage inductance, see the How2Power [Design Guide](#) and enter "leakage inductance" in the keyword search. And for more on magnetics design in general, see the [Design Guide](#), locate the "Design Area" category, and click on the "Magnetics" link.